The SVT IB remains based on the wafer-scale sensor of the ALICE-ITS3 upgrade in this case. The ALICE-ITS3 project is about to submit the second engineering run of its wafer-scale sensor and its timelines are compatible with those of the EIC project. In case of unforeseen future (sensor) delay, we will need to reprioritize ePIC efforts towards the ALICE-ITS3 sensor.

8.3.3.2 The MPGD trackers

Requirements

Requirements from physics: Micro-Pattern Gas Detector (MPGD) technologies have been chosen to complement the Si based tracking layers. MPGDs are relatively fast detectors able to provide precision space point measurements with good timing resolution, while also maintaining the overall conservative material budget that is required of the ePIC detector [45]. MPGDs will play a role in pattern recognition for central tracking system in the required pseudorapidity range of $-3.5 \leq \eta \leq 3.5$, and aid in PID reconstruction.

The EIC collider is expected to deliver collisions with bunches crossing every ∼10 ns [46], which will require the MPGD detectors to provide timing resolution of 10-20 ns to separate events from adjacent bunches. For ep collisions of 10 × 275 GeV, the DIS physics rate is expected to be around 500 kHz, while hadron and electron beam gas backgrounds rates are estimated to be 32.6 kHz and 3.17 MHz, respectively [47]. These rates are well within the rate capabilities of MPGDs. Combining the timing information from the MPGDs with information from the Si detectors will allow pattern recognition algorithms to discriminate between physics and background signals. In addition to providing hit information with good timing resolutions, the MPGDs will provide

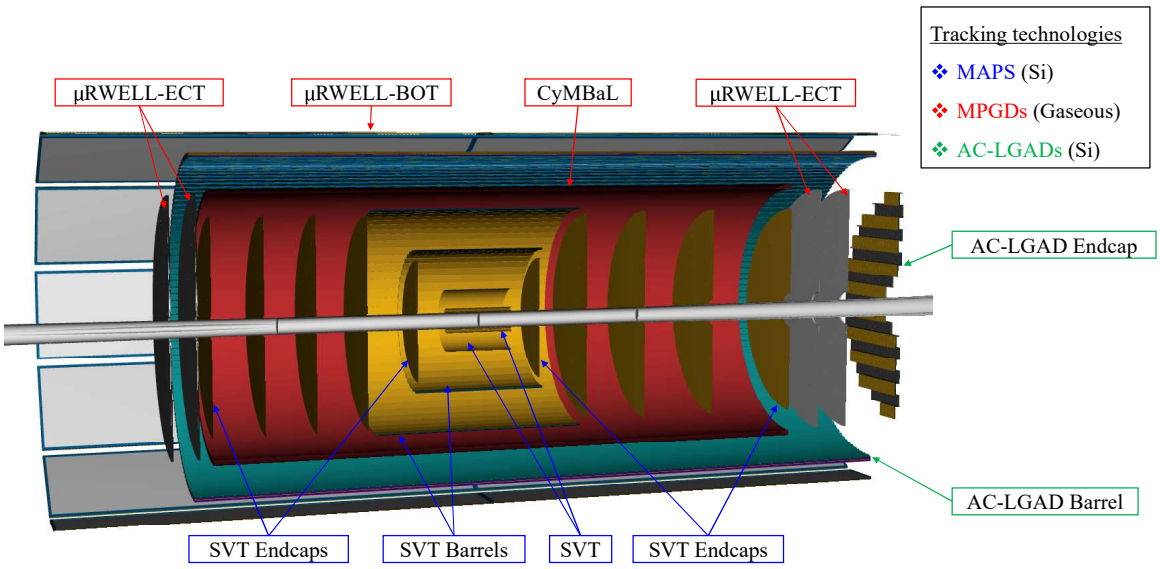

Figure 8.33: ePIC tracking subsystems.

additional hit points needed for robust track reconstruction. Early simulations showed that the number of hit points used in the track reconstruction reduced from around 6 hits near $\eta = 0$, to

only 3 hits at $|\eta| > 3$, due to tracks moving out of the acceptance of some of the Si layers. The ePIC endcap gaseous trackers, (µRWELL-ECT) were implemented to recover additional hits at larger η values. Figure 8.34 shows the average number of hits per event in the current ePIC tracking detector as a function of η for different momentum ranges. In this configuration the ePIC tracker measures at least 5 hits per event in the region ($|\eta| < 3.5$).
Finally, as detailed in the Yellow Report [45], the hpDIRC requires the track entering the PID volume to have good angular resolution (0.5 mrad at p = 6 GeV) in order to meet its performance requirements. This will be accomplished by providing the hpDIRC with precision hit points just before a particle enters its volume via the ePIC barrel outer tracker (µRWELL-BOT), and after it exits the hpDIRC volume via the first tracking layer of the barrel imaging calorimeter.

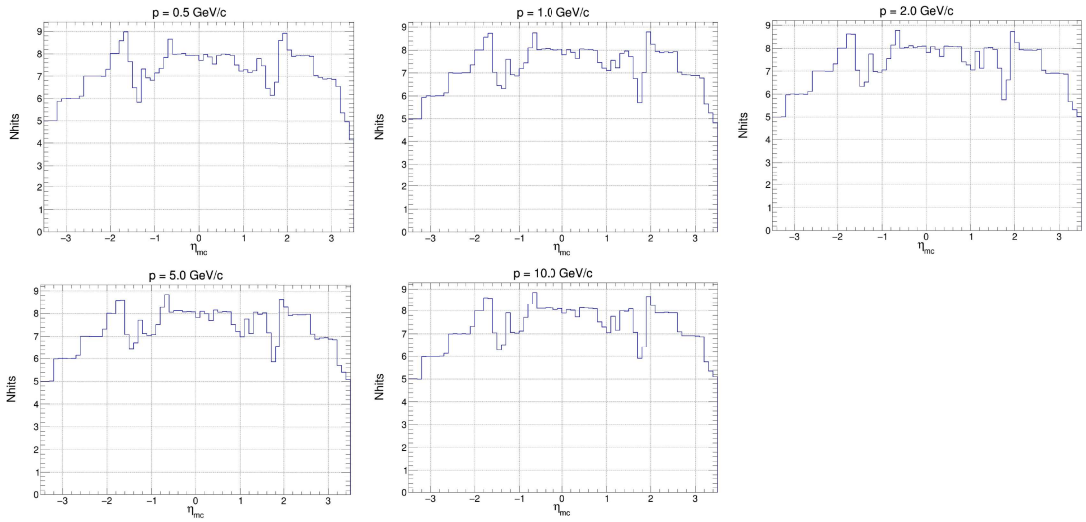

Figure 8.34: Total tracker hits vs. η for various momentum ranges (gitHub Repo).

Requirements from Radiation Hardness: Detailed simulation on radiation dose in ePIC has been performed. Figure 8.35 shows the estimate of hadron and EM radiation doses in ePIC simulation along with location of MPGD layers [47]. Table 8.5 shows the maximum estimated radiation dose from various sources for MPGD trackers at various locations with 10 years of running at top machine luminosity and 100% detector and accelerator efficiency based on e+p PYTHIA simulation. The MPGD trackers in ePIC will experience low radiation dose and based on past experience with MPGD trackers in various experiments [49–51] there will be negligible aging issues. The electronics will be mounted close to the MPGD trackers, and will be based on SALSA readout ASICs. It will also require specific DC-DC converter components able to stand the ePIC radiation and magnetic field levels. Both components are described in section 8.3.10 of this document.

Requirements from Data Rates: Table 8.6 shows hit rate per unit area for each MPGD subsystem in ePIC which is far lower than rate capability of MPGD detectors [52,53]. Table 8.7 shows the maximum hit rate experienced by a channel for various MPGD trackers in ePIC [47]. The rates are low enough for ASIC developed for MPGDs which can handle rate of 100 kHz/channel.

Justification The requirements cited above drives the necessity of using MPGD trackers at various locations of ePIC. MPGDs can be built over large area and their ability to handle high rates and

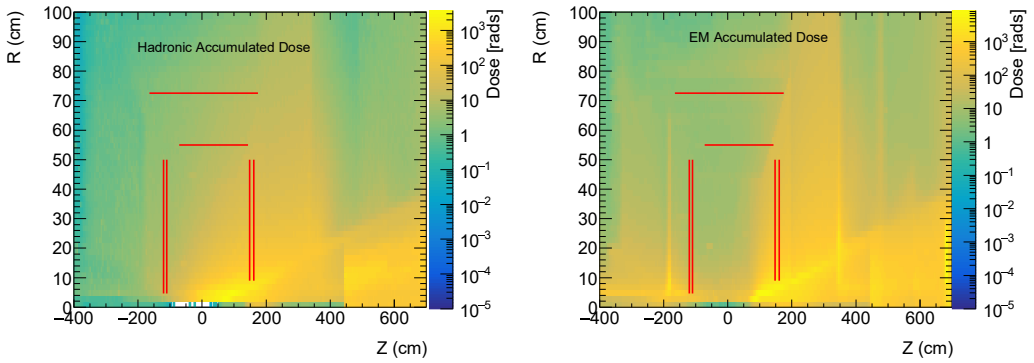

Figure 8.35: (*left*) EM radiation and (*right*) Hadron radiation dose estimate for minimum bias PYTHIA e+p events at 10x275 GeV at top machine luminosity for 6 months of running at 100% machine and detector efficiency [47]. The locations of MPGD trackers are shown by red lines [48]. (gitHub Repo).

MPGD tracker	EM Radiation dose [krad]	Hadron Radiation dose [krad]	1 MeV neutrons equivalent fluence [cm^{-2}]	1 MeV protons equivalent fluence [cm^{-2}]
CyMBaL	0.22	0.15	2.7×10^{10}	2.0×10^{10}
μRWELL-BOT	0.3	0.1	2.8×10^{10}	4.2×10^{9}
electron ECT	0.064	0.03	1.1×10^{10}	1.7×10^{9}
hadron ECT	0.87	0.23	3.0×10^{10}	8.5×10^{9}

Table 8.5: Maximum dose of radiation by different sources at MPGD tracker layers for e+p minimum-bias event at 500 kHz event rate for 10 years EIC running with 6 months run time per year and 100% efficiency [47].

MPGD tracker	DIS e+p rate [Hz/cm^2]	Hadron beam gas rate [Hz/cm^2]	Electron beam gas rate [Hz/cm^2]
CyMBaL	26.37	14.33	5.5
μRWELL-BOT	9.82	5.33	1.7
electron ECT	144.68	78.63	437
hadron ECT	1326.36	720	201

Table 8.6: Hit rate per unit area of various MPGD trackers for e+p DIS events at 10×275 GeV with $1.54\times10^{34}cm^2s^{-1}$ luminosity scaled from e+p DIS events at 18×275 GeV and $1.54\times10^{33}cm^2s^{-1}$ luminosity, 10 GeV electron beam gas and 275 GeV hadron beam gas

good spatial resolution makes them excellent candidate for large trackers.

Device concept and technological choice: The MPGD trackers are based on two different technologies and are described below

MPGD tracker	DIS e+p events [Hz]	Hadron beam gas [Hz]	Electron beam gas [Hz]
CyMBaL	3.68	0.05	4.78
μRWELL-BOT	2.76	0.04	4.78
electron ECT	9.2	3.56	102
hadron ECT	101.2	4.39	39.88

Table 8.7: Maximum hit rate by a single channel of various MPGD trackers for e+p DIS events at 10×275 GeV with $1.54 \times 10^{34}\text{cm}^2\text{s}^{-1}$ luminosity scaled from e+p DIS events at 18×275 GeV and $1.54 \times 10^{33}\text{cm}^2\text{s}^{-1}$ luminosity, 10 GeV electron beam gas and 275 GeV hadron beam gas.

CyMBaL: The role of the Cylindrical Micromegas Barrel Layer (CyMBaL) is to wrap around the SVT in its entire length to provide an additional hit point. Consequently, the main requirement is to have as little as possible acceptance gaps. In order to limit the impact on particle reconstruction in the outer detectors, CyMBaL has to be light in material budget, possibly less than $X/X_0 \sim 1\%$. CyMBaL (Figure 8.36a) is composed as a set of 32 Micromegas tiles arranged in a way to ensure full coverage in φ (8 modules) and in z (4 modules). The space envelope assigned to CyMBaL spans the range between 55 cm and 60 cm in radius and it is asymmetric in the longitudinal direction, covering the range -105 cm $< z <$ 143 cm. CyMBaL is designed in two symmetric halves that meet at $z = 19$ cm (due to the asymmetric keeping zone). In each half, the 16 modules are arranged in two cylinders, the inner one (in $|z|$) sitting at a radius of 55 cm and the outer one at 57.5 cm.
In order to limit the complexity of the detector production, the design is aiming at limiting the differences among the modules, possibly having only a single design for the module PCBs that will be assembled with different bending radii. The preliminary design of a CyMBaL module is

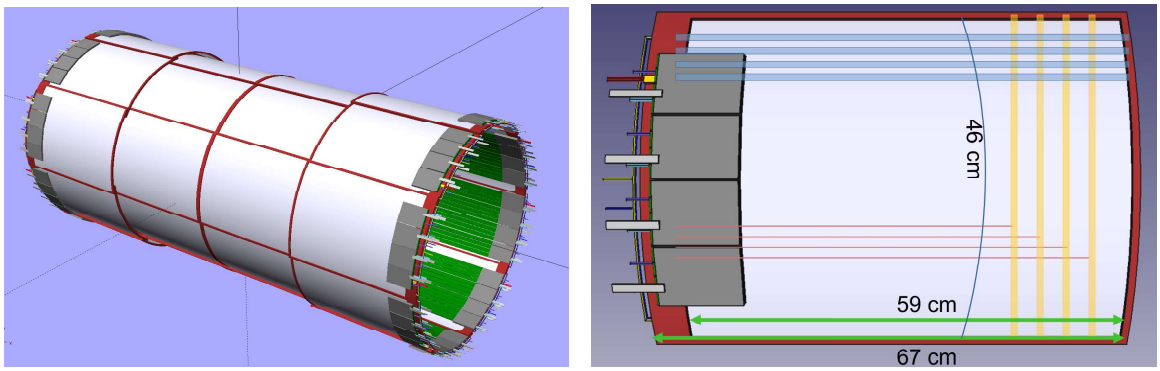

(a) **(b)**

Figure 8.36: [CyMBaL CAD model](a) CyMBaL CAD model showing the assembly of the 32 modules. (b)CAD model of a CyMBaL module. The light blue represents examples of readout strips measuring the $r \cdot \varphi$ coordinate (called Z-strips as they run along the z axis). The light yellow represents examples of readout strips measuring the z coordinate (called C-strips as they are arcs of a cylinder). The light red lines represent examples of trail lines to bring the C-strip signals to the FEBs. For the explanation of the services see the text.

shown in Figure 8.36b. A module is a cylindrical tile 48 cm wide (equivalent to about 50 degrees in the azimuthal direction) and 67 cm long, and the active region is about 46×59 cm^2. In the current design, the module dimensions allow for an overlap of 2.8 cm in the $r \cdot \phi$ direction and about 2 cm in z. The sensor is based on the bulk resistive Micromegas technology [54] with a 3 mm conversion gap.

The main purpose of the resistive layer is to share the charge, induced by the amplification, to neighboring strips in order to improve the spatial resolution. The resistive layer will also prevent sparks in the amplification region, although the expected particle rates are low and spark limitation would not be a major concern. The signal will be readout by orthogonal strips to provide a two dimensional information of the position of the charged particle crossing the sensitive area. The strips running along the longitudinal direction (therefore called Z-strips) will provide the $r \cdot \varphi$ measurement of the hit and they will be directly routed to the connector area. The strips running along the azimuthal direction (C-strips, C for cylindrical) will provide the z information of the hit and they will need to be connected with vias to routing trails to bring the signals to the connectors. The pitch of the readout strips will be $\sim$ 1 mm and the resistive layer will allow the charges to be shared among neighboring strips for a better centroid reconstruction. The total number of strips per module will be 1024 and they will be readout by four FEBs, each one equipped with $4 \times$ 64-channel SALSA chips. The module's frame will consists of carbon fiber hollow square beams and arcs of about 3 mm in size. Being hollow, these beams not only will provide the mechanical rigidity and support for the detector, but will be also used to distribute the gas inside the detector. As shown in Figure 8.36, the FEBs will be mounted at the two ends of CyMBaL to concentrate the material budget in just few areas. Low-mass micro-coaxial cables will be used to bring the signals from the modules to the FEBs: the inner modules will need cables of about 50 cm in length, while short (¡10cm) cables are sufficient for the outer modules. It is expected that the detector gain will be sufficiently high to overcome any noise induced by the additional capacitance of the cables.

µRWELL-BOT: ePIC MPGD Barrel Outer Tracker (µRWELL-BOT layer) is the outermost gaseous tracking layer installed in the barrel region of ePIC central tracker. The detector sits right

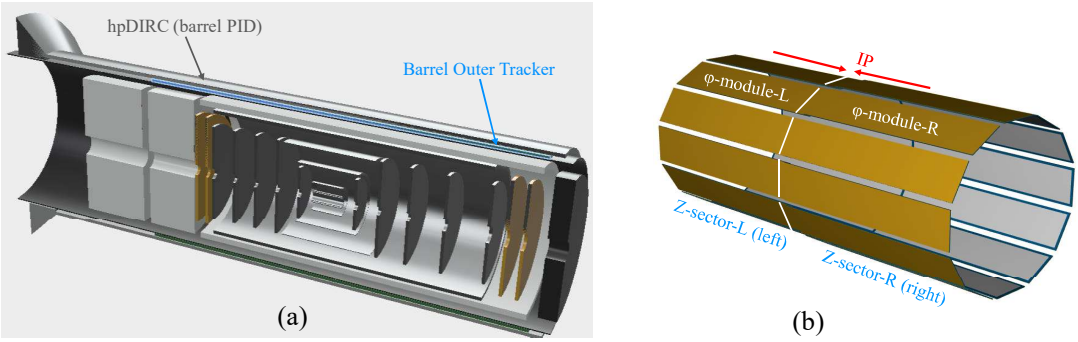

Figure 8.37: (a) µRWELL-BOT in ePIC central detector; (b) Arrangement of 24 µRWELL-BOT modules in dodecagon shape.

at a radius of 72.5 cm right in front of the high performance DIRC (hpDIRC) as shown in the layout at the top left of Figure 8.37. The tracker is split in two sectors (Z-sector) along the beam axis z. Each Z-sector is consists of 12 µRWELL-BOT rectangular modules (φ-modules) arranged in dodecagon shape to cover 2π acceptance in the azimuthal direction (φ) as shown in the top right of Figure 8.37. The µRWELL-BOT φ-modules are designed to match the hpDIRC acceptance in both z and φ as shown on the bottom right of Figure 8.37. Mechanical constraints associated to the detector support frames as well as the very limited space available for integration in the ePIC detector support frames result in an acceptance gap of $\sim$13% in φ and $\sim$1% in z. The material

budget X/X_0 of the detector is ∼1.5% in the active area but will becomes significantly higher at the edges of the detector where the front end electronics cards, cables and services are be located. The design of the full size μRWELL-BOT module engineering test article shown in Figure 8.43 developed as part of the Project Engineering Design (PED) effort based on thin-gap GEM-μRWELL technology (see paragraph section 8.3.3.2 and Figure 8.44) is complete and the fabrication of the chamber is scheduled for the first half of 2025.

μRWELL-ECT: Monte Carlo simulations show that the endcap regions of the ePIC detector experience the highest backgrounds in the experiment and charged particle tracking requires several hit points in the $|\eta| > 2$ region for good pattern recognition. To optimize the ePIC baseline tracker design, two planar Micro-Pattern Gaseous Detectors (MPGD) disks, with a central hole for the beam pipe are located both in the hadronic and the leptonic sectors (see the right drawing of Figure 8.38). The ECT disks geometrical envelope is reported in Table 8.8. It takes into account the integration constraints within the ePIC detector and the beam pipes dimensions. As shown in the left drawing of Figure 8.38, the hadron and lepton beam pipes slightly diverge from the interaction point. Therefore the ECT inner radii are calculated taking into account the envelope radii and their center offset. For simplicity the inner radius if fixed by the largest of the two values calculated for the disk located at the larger z position at each endcap region. As a result the two lepton disks located closer to the interaction point, will have a smaller inner radius than the two hadron disks (4.65 cm vs 9 cm) as they are located closer to the interaction point, while the outer radii of 50 cm are equal for all the four disks and are fixed by the available volume inside the ePIC detector. The ECT disks envelope also includes the MPDG gas frames of 1.5 cm thickness, and a

MPGD Disk	Longitudinal location z (cm)	Outer Radius (cm)	Inner Radius (cm)	Outer Active Area Radius (cm)	Inner Active Area Radius (cm)
HD MPGD 2	161	50	9	45	10.5
HD MPGD 1	148	50	9	45	10.5
LD MPGD 1	-110	50	4.65	45	6
LD MPGD 2	-120	50	4.65	45	6

Table 8.8: The ECT disks geometrical envelope and active areas dimensions.

3.5 cm outer service ring, to locate services and electronics front-end boards. The resulting active area dimensions of the disks are also reported in Table 8.8 and the corresponding angular and pseudorapidity acceptances are reported in Table 8.9. The final active ranges in pseudorapidity are $2.0 < \eta < 3.3$ for the hadron sector and $-3.6 < \eta < -1.7$ for the lepton sector, constrained by the available space.

MPGD Disk	$\|\theta\|$ min (deg)	$\|\theta\|$ max (deg)	$\|\eta\|$ min	$\|\eta\|$ max
HD MPGD 2	3.7	15.5	2.0	3.4
HD MPGD 1	4.0	16.9	1.9	3.3
LD MPGD 1	3.1	22.1	1.6	3.6
LD MPGD 2	2.8	20.4	1.7	3.7

Table 8.9: The ECT disks angular and pseudorapidity acceptance.

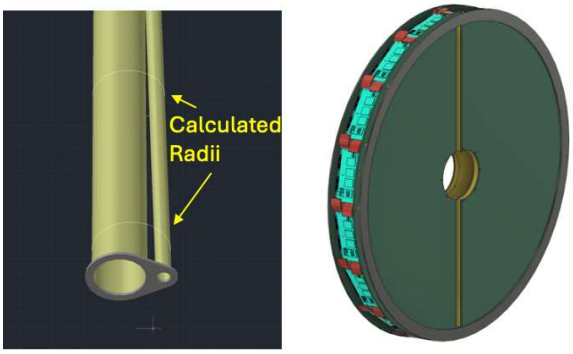

Figure 8.38: Left: Hadron and lepton beam pipes slightly diverge from the interaction point. The ECT inner radii are calculated taking into account the envelope radii and their center offset, the hadron beampipe forming a larger angle with the z axis. Right: layout of a couple of μRWELL-ECT disks.

A GEM-μRWELL hybrid technology [55] with XY 2D readout, similar to the one described for the μRWELL-BOT and shown in Figure 8.44(b), has been chosen to match all the performance requirements.The main difference is related to the drift region gap, which is 3-6 mm wide to ensure an intrinsic efficiency higher than 97-98%. A 2D strip read-out COMPASS-like scheme, where the charge is collected by XY orthogonal strips located on two different printed circuit board (PCB) layers, has been chosen. The strip widths of the two coordinates must be optimized (in a ratio of about 1:3) to balance the signal amplitude in the two dimensions, since the upper layer strips screen the charge collected on the lower ones.

The XY Cartesian readout scheme was preferred over the Rφ geometry for two reasons: i) the high radial strip density at the center hole and ii) the possibility offered by the XY geometry to route all the strips to connectors located on the outer service ring. The cathode and the 2D readout PCB are supported by a 3 mm thick honeycomb structure to minimize the detector material budget, which amounts to $0.85\% X/X_0$ in the active region.

Front End Electronics (FEE): To meet the requirement of streaming readout new front-end chips for MPGD trackers in ePIC are being developed by Sao Paulo Universities and CEA Saclay IRFU. The SALSA chip, which associates an analog front-end adapted to MPGD detectors, an ADC per channel with a 50MS/s digitization rate on 12 bits, and a data processing unit, has the following characteristics:

- 64 channels with large input capacitance range (up to 1 nF), optimized for 50-200 pF.
- Large range of peaking times: 50-500 ns.
- Large gain ranges: 0-50 to 0-5000 fC.
- Large range of input rates, up to 100 kHz/ch.
- Reversible polarity.

Other components. The **gas mixing unit** will be a critical component of the MPGD trackers. The mixing unit preferably will use Mass Flow Controllers based on Proportional-Integral-Derivative (PID) control systems. Furthermore, the mixing unit should be able to mix either two or three different inert gases depending on the final composition of the operating gas. The preferred mixture for

CyMBaL is Ar-isobutane (95:5) see Figure 8.42, however if concern is raised for flammability of this gas mixture then a three gas mixing unit will provide the possibility of adding a third gas (preferably CO_2) at the expense of isobutane. This will help in maintaining stability by operating the detector at lower voltage (due to the isobutane component), make the gas faster and non-flammable (due to the CO_2) component. Additionally **sensors** will be installed to monitor the temperature, pressure and humidity close to MPGD modules and if possible also to monitor temperature of incoming and outgoing gas to give an idea of heating of gas volume inside detector itself. The High Voltage Power Supplies (HVPS) are another important component for MPGD trackers to bias the detector. The preferred way of biasing each module of MPGD tracker is by using voltage divider. The HVPS will have low ripple (< 5 mVpp) to reduce noise from HVPS along with the capability of monitoring current drawn by the detector.

Performance The MPGD tracking detectors share 2D spatial resolutions performances better $\simeq 150$ μm, timing resolutions of the order of $10 - 20$ ns, rate capability better than 10 kHz/cm^2, and detectors response not impacted by temperature instabilities, which may be compensated in the calibration procedures. The radiation hardness of the components material will sustain the doses reported in Table 8.5. The specific performances of each MPGD subsystem are reported in the following.

CyMBaL: The CyMBaL design aims at providing complete azimuth (φ) coverage. Along the longitudinal direction where the two halves of the system meet, only $\sim$3 cm will not be covered. CyMBaL modules are expected to provide a hit spatial resolution around 150 μm with a time resolution of $10 - 20$ ns. The modules are expected to operate with efficiencies above 95%. The magnetic field, being orthogonal to the drift field, will cause the primary electrons to drift away from the electric field lines, the so called Lorentz angle. This effect could degrade the $r \cdot \phi$ resolution. To limit the Lorentz angle, the module's drift fields will be set at about 3 kV/cm and adjusted among modules to account for possible longitudinal variation of the magnetic field.

μRWELL-BOT: The barrel outer tracker will provide hit space point resolution better than 150 μm on average in the eta range of $-1 \leq \eta \leq 1$ and 100 μm in the azimuthal direction and a timing resolution of $\sim$10 ns. The tracker has an acceptance gap of 13% along φ because of space constraints imposed by the limited space in the ePIC detector. The tracker will operate at a nominal efficiency of $\sim$95%. As shown in Figures 8.6 and 8.7, the particle rate per unit area and per readout channel is very low and will not pose any challenge in term of tracking performance, safety operation and long term stability of the μRWELL-BOT trackers for the lifetime of the ePIC detector.

μRWELL-ECT: The MPGD-ECT disks are designed to provide intrinsic spatial resolution for perpendicular tracks less than 150 μm. Technological solutions and data analysis procedures exist to guarantee similar performances also for inclined or curved tracks. The active area of the detector has a material budget less than 1% in units of radiation length (X_0) and will cover all azimuthal angels in the polar region specified in Table 8.9. A time resolution in the $10 - 20$ ns range is achievable using the gas mixtures described above. A single disk efficiency of $\simeq$ 96–97% is required to provide 92–94% combined efficiency for two disks in the same region.

Implementation:

Services: The MPGD tracking detectors subsystem are divided in different modules, each one requiring: gas supply lines and outlet, front end boards (FEB) connected to 5-line optical fibers (VTRX+) for data transfer to the RDO, low voltage lines (four lines for each FEB: one pair for the 1.8 V and one for the 3.3 V.), high voltage cables, temperature and humidity sensors and cooling in and out lines. Studies on the type of cooling and possible implementation in a serialize distribution will be done in synergy with the other subsystem of ePIC.

The service requirements for each MPGD tracking subsystem is summarized in Table 8.10.

Subsystem	**CyMBaL**	**μRWELL-BOT**	**μRWELL-ECT**
Number of Modules	32 Micromegas tiles	24 GEM-μRWELL φ-modules	4 GEM-μRWELL disks
Gas supply lines per module	1 in / 1 out	1 in / 1 out	8 in / 8 out
Number of FEB per module	4	14	32
Low voltage lines per module	16	56	128
High voltage lines per module	2	1 (or 4)	16
Cooling lines per module	1 in / 1 out	1 in / 1 out	4 in / 4 out
VTRX+ lines per module	4	14	32

Table 8.10: Services requirements for the three MPGD tracking subsystems.

Subsystem mechanics and integration: CyMBaL integration and mechanics rely on the central tracker global support structures. CyMBaL modules will be connected to the support structure. For μRWELL-BOT, the support structure connecting the carbon fiber tube and EM-Cal will serve as μRWELL-BOT and HP-DIRC support structure whereas for μRWELL-ECT, the outer ring of each disk hosts all the services listed in Table 8.10. The FEB are mounted perpendicularly to the disks.

Because of the divergence of the beam pipes, the disks cannot longitudinally slide along them but need to be shaped in sectors to be mounted around the pipes. Moreover, as the width of the Cu-kapton foil base material for the MPGD detectors restricts one dimension to about 550 mm, an implementation of the endcap trackers would consist of two half-circular disks with "D-shaped" cut-outs for the beam pipe, eventually sub segmented in four quadrants. As sketched in Figure 8.39, the disks integration and mechanics rely on the central tracker global support structures, using the same layout of the Silicon trackers. The MPGD-ECT disk are the most outer elements in the endcap region and the last to be installed in the mounting scheme of the tracking system.

Calibration, alignment and monitoring: The three MPGD subsystems will generally follow similar calibration, alignment and monitoring procedures. There are two main calibration tasks that have been identified. The first is to determine the optimal HV settings for the MPGDs, which will be determined through efficiency scans. These scans will be performed prior to data taking campaigns and after changes in running conditions (e.g. changes in gas composition). The second calibration task is to determine pedestal values and the common noise to be subtracted from the ADC samples, which will be determined through dedicated calibration runs. To meet the overall ePIC tracking performance precise knowledge of the tracking detector positions will need to be known. The alignment of the MPGD modules will be surveyed and entered into a database before integration. This information will be used to establish a starting point for the software alignment, which will be based on track reconstruction with and without magnetic field applied and

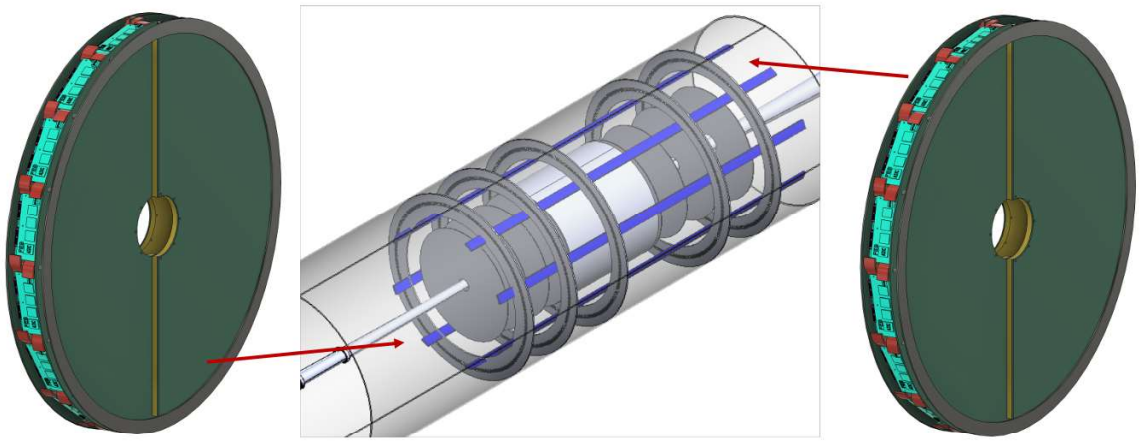

Figure 8.39: Integration of the MPGD-ECT disks in the ePIC detector.

will involve all of the ePIC tracking detectors. To assure that the MPGD detectors are performing optimally there are several criteria that will be monitored, which include the gas composition, the environmental conditions near the MPGDs (e.g. temperature, humidity and pressure), currents drawn by the MPGD layers from the power supply and general detector performance. Changes in the environmental conditions can be addressed by adjusting the detector gain via a feedback loop. The currents drawn by each high voltage channel will be read out and logged with a frequency of about 1 Hz. Additionally, we will need to monitor and log the low voltage currents and FEB temperatures. Not only will this allow us to monitor for abnormal values, but also implement automatic safety measures should a particular value fall outside of an acceptable range. Finally, during data taking we will monitor basic detector performance parameters such as hit occupancy maps, 2D efficiency, signal amplitude and timing distributions will be constantly monitored.

Status and remaining design effort: R&D and PED

CyMBaL: The resistive Micromegas technology has been extensively used in nuclear and particle physics experiments. In particular, 1D-readout cylindrical Micromegas tiles are in use at JLab in the Barrel Micromegas Tracker (BMT) of the CLAS12 experiment since 2017 [56], in experimental conditions which are more challenging than those expected at the EIC. The main focus of the ongoing R&D is to upgrade the BMT technology to 2D readout. In order to limit the number or readout channels, the R&D also focus on exploiting the charge sharing through the resistive layer and using $\sim$1 mm pitch readout strips. Several combinations of strip readout patterns together with layers of different resistivity have been tested in a beam test in MAMI in 2023. Further studies are ongoing with the cosmic rays test bench in Saclay and an additional beam test at CERN is planned for 2025. The design of a CyMBaL module prototype has begun and its production and tests are expected to be completed in 2026.

μRWELL-BOT: The R&D phase for the development of the μRWELL-based trackers for EIC detector was completed in summer 2023 and transitioned into project engineering design (PED) effort. The goal for PED effort is to develop a full size thin-gap GEM-μRWELL engineering test article as a beta version of pre-production φ-module of μRWELL-BOT tracker in ePIC detector. The design effort including the CAD drawings of all mechanical parts that is frames and support structures as well as the sensitive devices such as the GEM foil, the μRWELL and the U-V strip

readout PCB is in advanced stage and expected to be completed by the end of 2024. The fabrication of the full size engineering test article will take place during the first half of 2025. The second half of the year 2025 will be dedicated to a full characterization of the prototype on a cosmic test bench setup and in beam at the CERN NA H4 beam test area including test in its 1.5 T GOLIATH magnet to study the performance of the detector in a magnetic field strength similar to the one expected from the ePIC magnet. The PED effort to develop the μRWELL-BOT module including a detailed review of the design choices and options, the timeline and outlook for the completion of the engineering test article effort.

μRWELL-ECT: Disk design and modules segmentation is undergoing. The choice of the connectors will have in impact on the final strip pitch and the total number of read-out channels for each disk: usage of Hirose connectors (140 pins for 126 channels) would limit the maximum number of connectors and read-out channels if compared with obsolete Panasonic ones. Segmentation of the disks in four quadrants may avoid the use of a support structure for the GEM foil. A final decision on the final layout will be based on the results of prototype testing. Figure 8.40 shows some design details under investigation.

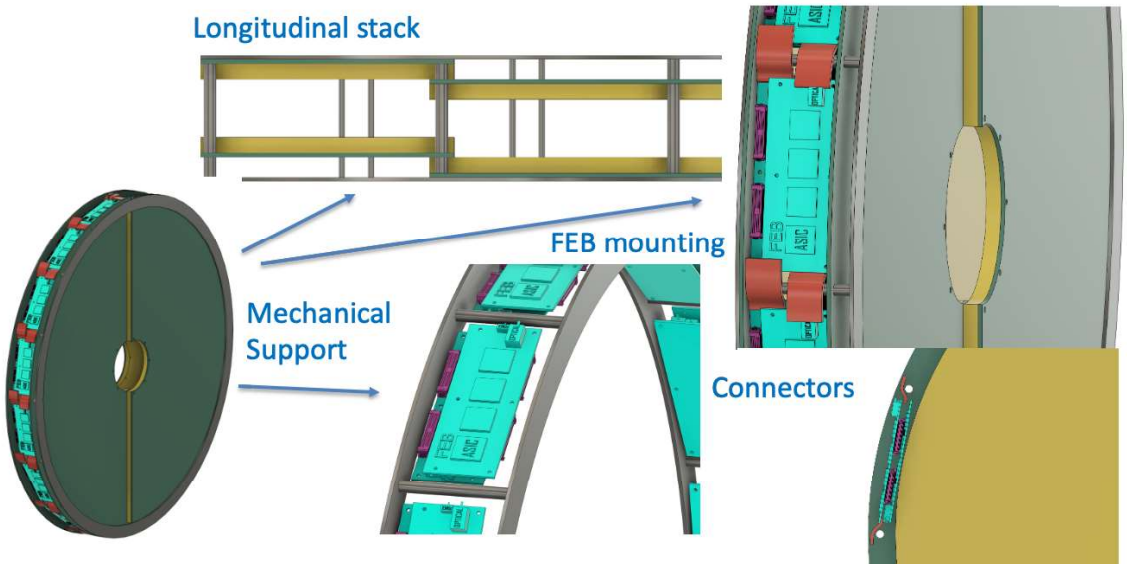

Figure 8.40: Design details of MPGD-ECT disks

Environmental, Safety and Health (ES&H) aspects and Quality Assessment: Considering MPGD consortium is composed of international collaboration so each production site for module assembly will follow guidelines of their local government to be in compliance with ES&H requirements. This include minimizing wastes during assembly procedure and disposal of harmful wastes in safe manner as directed by local government along with general electric and mechanical safety. During final integration of the detector subsystem at BNL , scientists and technicians will follow DOE guidelines as directed by BNL ES&H department.
The Quality Assessment protocol will cover the entire production lane of MPGD detectors. The readout PCBs will be assessed for mechanical precision and electrical continuity. The resistive layers will be checked for uniformity. During each step of the assembling, electrical continuity and high voltage capability of the different electrodes will be tested. Once the assembly of the module is finished, the module is checked for gas leakage and HV stability before bringing it outside of the

clean rooms. Each finished detector will be then tested with cosmic rays in dedicated test benches. In these tests, the main parameters that will be studied for each module are the noise levels and the number of dead channels, efficiency and effective gain uniformity over the detector active area . A database will be used to log all the information and results for each produced module.

Construction and assembly planning. Each of the MPGD detectors share a similar construction, assembly and QA timeline for having the detectors arrive at BNL in late 2029. This general timeline is shown in Figure 8.41.
The construction and assembly of the MPGD subsystems will take place at various places. CEA-Saclay will be the main production site for CyMBaL modules, while the readout PCBs will be produced by industry partners. At Saclay, all the remaining parts of the production process will be realized. The resistive layer will be added using serigraphy and the low-tension micromesh will be added using the bulk process [57], which will be performed in the Saclay MPGD Lab. The curving and mechanical integration of the final detector will be done in a dedicated clean room.
CERN will serve as the primary source for µRWELL and GEM foils, as well as the readout PCBs for the µRWELL-BOT and µRWELL-ECT detectors. Other components, such as the frames, will be produced by industry partners. The production sites of the µRWELL-BOT subsystem are Jefferson Lab, Florida Institute of Technology and University of Virginia whereas INFN and Temple University will be in charge of the µRWELL-ECT subsystem.

A set of technical documents will be developed for each MPGD sub-detector, ensuring that all modules are produced under consistent conditions, using appropriate infrastructure, and following standardized procedures for construction and quality control testing. Each production site will procure and inspect the components separately. It is crucial that all production sites are equipped with suitable clean room infrastructure for the construction and assembly of their respective µRWELL modules, as well as identical instrumentation for a standardized component inspection and module characterization. Each of the institutes will be responsible for the construction and characterization of their respective µRWELL modules (+ spares). The equipment needed for each subsystem will listed in in appendix before the next draft. Each institution will leverage its existing MPGD infrastructure (clean room and detector lab and existing equipment) to minimize instrumentation costs but will upgrade where needed to meet the more demanding requirement of µRWELL technology assembly.

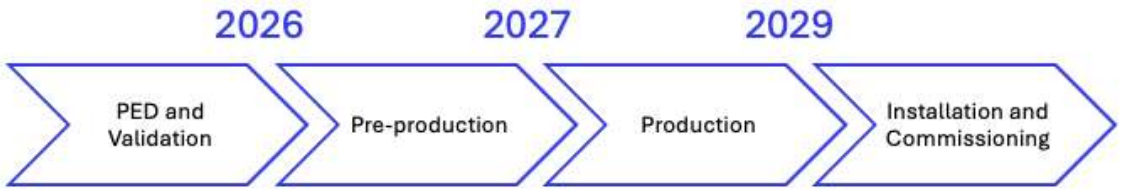

Figure 8.41: General overview ePIC MPGD tracker construction and assembly timeline.

Collaborators and their role, resources and workforce :

CyMBaL: Design, production and tests will be lead by CEA Saclay.The details of the workforce, role and resources for each subsystem will be added in appendix before the next draft.

μRWELL-BOT: Jefferson Lab, Florida Institute of Technology, and the University of Virginia will participate in the construction, assembly, and characterization of μRWELL-BOT φ-modules to ensure timely mass production. Each of the three institutes will be responsible for the construction and characterization of eight μRWELL-BOT φ-modules (+. The essential equipment needed for each institute are listed in Tab. 8.12. Wherever possible, existing equipment from the collaborating groups will be utilized to minimize instrumentation costs. They will collaborate to develop a set of technical documents, ensuring that all modules are produced under consistent conditions, using appropriate infrastructure, and following standardized procedures for construction and quality control testing. All components of a μRWELL-BOT φ-module will be designed by Jefferson Lab, however, each production site will procure and inspect the components separately. It is crucial that all three production sites are equipped with suitable clean room infrastructure for the construction and assembly of μRWELL-BOT φ-modules, as well as identical instrumentation for a standardized component inspection and module characterization. Each of the three institutes will be responsible for the construction and characterization of eight μRWELL-BOT φ-modules (+ spares). The essential equipment needed for each institute are listed in Table 8.12. Each institution will leverage on its existing MPGD infrastructure (clean room and detector lab and existing equipment) to minimize instrumentation costs but will upgrade wherever possible to meet the more demanding requirement of μRWELL technology assembly. The personnel effort, expressed as a percentage of research time over the duration of the project, at each institute is provided in Tables 8.13, 8.14, 8.15.

μRWELL-ECT: Temple University and INFN Roma Tor Vergata — will participate in the design, production, assembly, and characterization of μRWELL-ECT disks, with the engineering support from Jefferson Lab and the collaboration of INFN LNF MPGD group lead by Gianni Bencivenni, inventor of the μ-RWELL technology. INFN Roma Tor Vergata will focus on the two hadron disks while Temple University will be in charge of the lepton disks. Each of the two institutes will be responsible for the construction and characterization of 4-8 μRWELL-ECT modules, depending on final design. The essential equipment needed for each institute are listed in Table 8.11. Wherever possible, existing equipment from the collaborating groups will be utilized to minimize instrumentation costs.

Risks and mitigation strategy: Based on past experiences with MPGD technology following risks and mitigation strategies are identified.

- Delay in production of MPGD foils at CERN is the biggest risk. Considering this it has been decided to place procurement request well in advance to provide enough time to procure the MPGD foils. Additionally there is possibility of using additional person power and also prepare additional set up for assembling each module in each assembly sites so that at least 2 modules are assembled at the same time.
- Minor risk of higher humidity content within the MPGD modules is possible however it can be mitigated by flowing gas at higher rate.
- It is possible that the gain provided by any of the MPGD module after installation in experimental hall is lower than what has been estimated during QA. This can be mitigated either by increasing the content of primary ionized gas in gas mixture or increasing the high voltage on MPGD electrodes without affecting detector stability.

Additional Material:

Gas choice: MPGDs will preferably operate with a mixture of argon-isobutane 95:5. This choice is being driven by two factors. On the one hand, MPGDs will operate in a solenoidal magnetic field of up to 2 T, while the drift electric field will be in the radial direction. This induces a Lorentz force on the primary electrons moving them in the azimuthal direction. In order to limit the effective angle of the resulting drift velocity with respect the electric field, one should aim at using a gas mixture that has a low electron drift velocity. A comparison of the Lorentz angle versus the drift

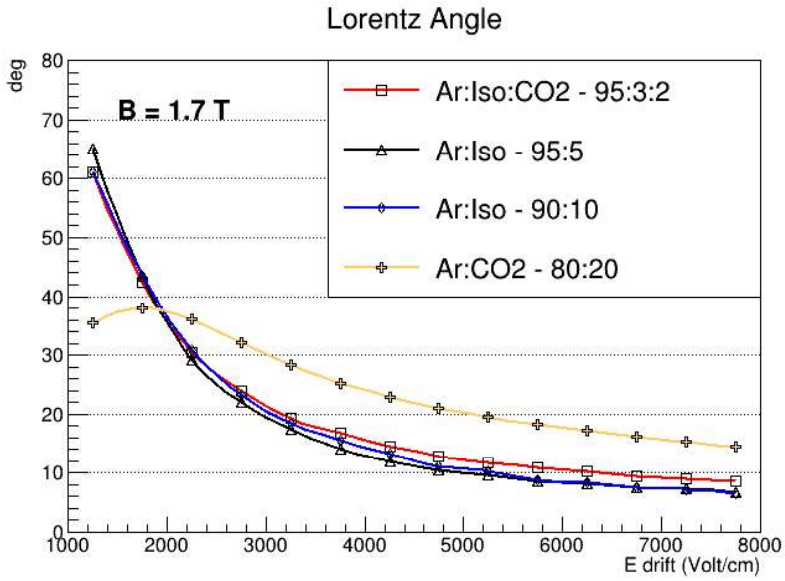

Figure 8.42: Comparison of the Lorentz angle as a function of the drift field for several gas mixtures. This study was done using Magboltz in Garfield++ [58].

filed among several argon based gas mixtures, commonly used in MPGD applications, is shown in Figure 8.42. One can see that in a 1.7 T magnetic field, an with drift voltages higher than 3 kV / cm, the Lorentz angle for Ar:Isobutane 95:5 mixture is lower than 20 degrees. On the other hand, the gas mixture must provide enough gain to ensure a good signal-over-noise ratio. Gases with a high fraction of argon ensure enough primary electrons and achieve high gains.

μRWELL-BOT φ-module design: is a large rectangular MPGD detector based on the thin-gap GEM-μRWELL hybrid detector concept described in detail in 8.44. The detector has an active area of 1700 mm × 330 mm and an overall dimension of 1815 mm × 360 mm and a thickness of 2 cm including the on-detector front end electronic boards (FEB cards) and cables and services. The thin-gap concept, defined by smaller drift gap of ∼1 mm in the drift region of the detector, combined with the double amplification with GEM and μRWELL structures and the proper choice of gas mixture guarantees a high performance the detector in all aspects satisfying the main requirement of the ePIC tracker such as a detector efficiency above 95%, a timing resolution better than 10 ns and space point resolution better than 150 μm on average in the pseudorapidity range of $-1 \leq \eta \leq 1$.

Thin-gap GEM-μRWELL hybrid detectors: Thin-gap GEM-μRWELL hybrid technology [59] was developed to satisfy the requirements of MPGD in term of space point and timing resolutions as well as detection efficiency above 95% and stable operation condition in the full angular

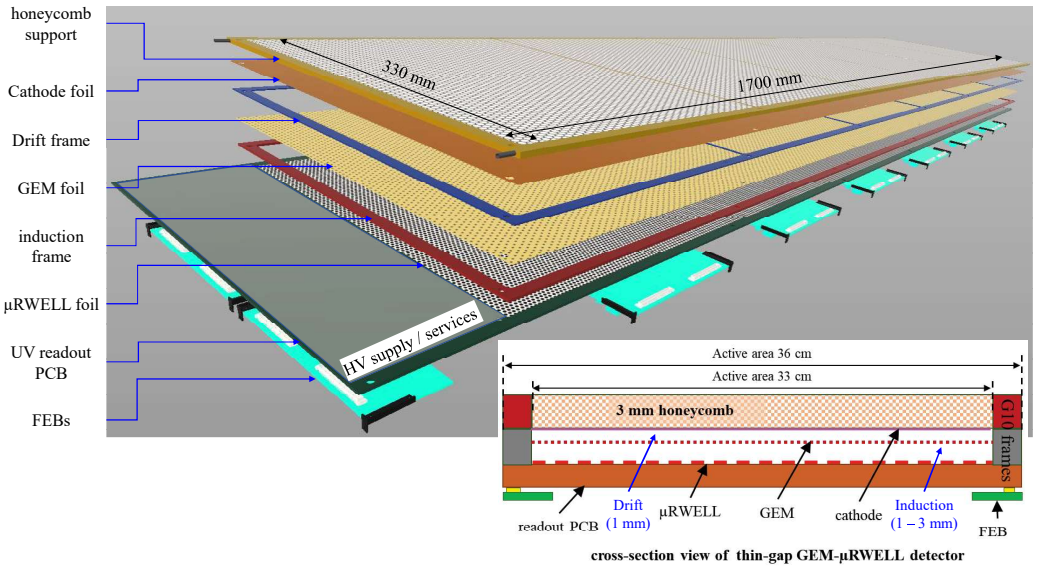

Figure 8.43: Exploded 3D view of the CAD design of the µRWELL-BOT φ-module with a breakdown of its essential sensitive items. *Bottom right:* Cross section view of the detector.

2460 acceptance of the ePIC detector. Three distinctive features are implemented in a thin-gap MPGD detector:

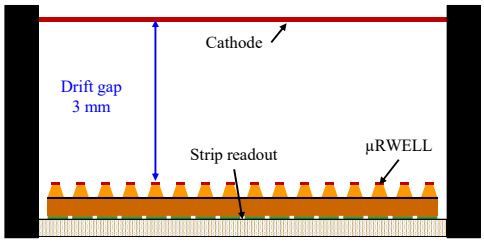

(a)

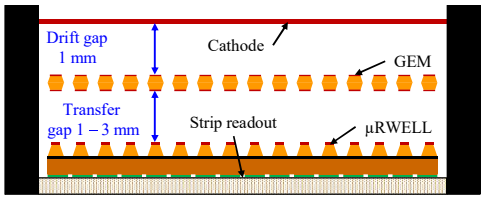

(b)

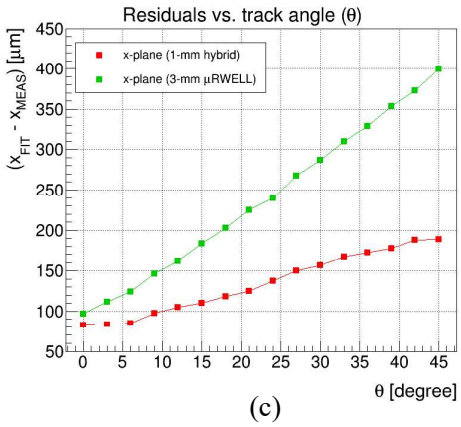

(c)

Figure 8.44: (a) Cross sectional view of a standard 3-mm gap µRWELL detector; (b) Cross sectional view of a 1-mm gap thin-gap GEM-µRWELL hybrid detector; (c) Spatial resolution as a function of the angle of impinging particle for standard gap µRWELL prototype (green) and for thin-gap GEM-µRWELL detector (red).

1. **Thin gap drift:** The basic idea of a thin-gap MPGD is to minimize the thickness of gas volume in the ionization region between the cathode and the first amplification stage of detector from the 3 mm typically used in a standard MPGD to ∼1 mm gap as shown on the two cartoons (a) and (b) of Figure 8.44). A smaller gas volume reduce the length of the ionization trail left by the particles traversing the detector at large angle. This, subsequently minimize the impact on the degradation of the spatial resolution.

2. **Hybrid amplification:** To recover from the smaller total charge produced in the ionization region due to the smaller gap, a higher gain from the amplification layer is needed. An optimal way to achieve large gain is to use a two-stage amplification with hybrid MPGD structures composed of a GEM foil used as pre-amplification and the µRWELL layer for the second amplification. A second advantage with the hybrid amplification is the flexibility to safely operate the detector at large gain.

3. **2D capacitive-sharing strip readout:** Capacitive-sharing readout structure is critical for thin-gap MPGDs to achieve required spatial resolution performance. Performance of µRWELL detector implementing capacitive-sharing 2D-strip readout is described in detail in [60]. For thin-gap µRWELL-GEM hybrid detector, without capacitive-sharing structure, smaller strip segmentation (with pitch $\leq$200 µm) would be required to achieve the the required spatial resolution. One can achieve same level of spatial resolution with larger pitch $\geq$1 mm) capacitive-sharing strip readout and therefore reducing the number of electronics channel by more than a factor 5. This represents a significant cost saving and reduction of the volume of cabling, services regarding the complexity of integration and maintenance for experiment.

The plot (c) of Figure 8.44) shows some preliminary results from beam test studies of the improvement of the spatial resolution as a function of the angle of incoming particles with the thin-gap (red curve) µRWELL-GEM hybrid prototype compared to the standard gap µRWELL prototype. Detailed description of the beam test setup and additional performance results will be provided in Appendix in future version.

Table 8.11: Main equipment required in the production site and availability at sites.

Equipment	**Purpose**	**INFN Roma Tor Vergata**	**Temple University**
ISO7 cleanroom	Inspection & Assembly	y	y
Stretcher system	Construction process	y	n
Ultrasonic Cleaner	GEM frame prep	n	y
Fume hood	GEM frame prep	y	y
Microscope	GEM visual inspection	y	y
Giga-Ohm insulation meter	GEM electrical inspection	y	n
HV box	GEM electrical cleaning	y	n
Oven	Construction process	y	n
Electronic instrumentation	Module characterization	y	n
Gas supplies	Module characterization	y	n
Shipping containers	Transport b/w sites	y	n

Table 8.12: Main equipment required in the production site and availability at sites

Equipment	Purpose	JLab	UVA	FIT
ISO7 cleanroom	Inspection & Assembly	y (need upgrade)	y	y
Stretcher system	Construction process	n	y	n
Assembly system	Assembly process	n	n	n
Isonic Ultrasonic Cleaner	GEM frame prep	n	y	n
Fume hood	GEM frame prep	n	y	n
Microscope	GEM visual inspection	n	y	y
Giga-Ohm insulation meter	GEM electrical inspection	n	y	y
HV box	GEM electrical cleaning	n	n	n
Oven	Construction process	n	n	n
Electronic instrumentation	Module characterization	y (partial)	n	y
Gas supplies	Module characterization	y	n	y
Shipping containers	Transport b/w sites	n	n	n

Table 8.13: UVa Personnel Effort (%FTE)

Personel	Effort
Faculty	25%
Research Scientist	50%
Graduate Student	50%
Graduate Student	50%
Undergraduate Student	25%
Technician	50%

Table 8.14: FIT Personnel Effort (%FTE)

Personel	Effort
Faculty	20%
Graduate Student	50%
3 Undergraduates	10%
2 Technicians	100%

8.3.4 Particle Identification

In addition to tracking and calorimetry, Particle IDentification (PID) is a crucial component of the ePIC experiment's physics program. The identification of stable particles is achieved either by analyzing the way they interact, or by determining their mass measuring their velocity and momentum simultaneously. The difference in interaction is primarily used for identifying leptons, photons and neutral hadrons, which leave very different signatures in the electromagnetic calorimeters. Charge hadrons cannot be distinguished by their interaction in the calorimeter, but their velocity can be measured using dedicated time-of-flight and Cherenkov detectors. All dedicated ePIC PID detec-